Janzen-Connell effects and habitat-induced aggregation synergistically promote species coexistence

Daniel J. B. Smith*
Department of Integrative Biology
University of Texas at Austin, Austin, TX USA

*Corresponding author: smithdj4@utexas.edu

Keywords: Coexistence theory; Janzen–Connell effects; conspecific negative density dependence; dispersal; habitat heterogeneity; competition; spatial ecology; tropical forests; niche partitioning; stabilization mechanisms.

Abstract

Janzen–Connell (JC) effects, habitat partitioning (HP), and dispersal limitation are three processes thought to shape tropical forest diversity and patterns of species aggregation, yet how they jointly influence species coexistence remains poorly understood. I analyze a spatially explicit model that incorporates all three processes, tracking propagules subject to habitat filtering and conspecific density dependence. The model shows that dispersal limitation and habitat filtering interact with JC-effects in qualitatively different ways. Aggregation driven by dispersal limitation weakens the ability of JC-effects to maintain coexistence, whereas when JC-effects and HP operate together in spatially autocorrelated habitats, richness increases with conspecific aggregation. JC-HP interactions strongly depend on habitat spatial structure. If habitats are not spatially autocorrelated, JC-effects and HP minimally interact (or act antagonistically when coupled with dispersal limitation) and do not maintain high species richness. However, when habitats are positively autocorrelated the two mechanisms act synergistically. To explain these patterns, I introduce a novel metric — the spatial JC–HP covariance — which quantifies how strongly JC-effects are concentrated in favorable versus unfavorable environments, providing a direct measure of the extent to which JC-effects and HP synergistically promote coexistence.

Introduction

Explaining how tropical forests sustain extraordinary levels of species diversity remains a central challenge in ecology. The difficulty stems from the competitive exclusion principle: without interspecific niche differences, the species with the highest fitness should exclude all others (Hardin, 1960; Levine & HilleRisLambers, 2009). This puzzle has motivated decades of empirical and theoretical work to identify the mechanisms that allow stable coexistence.

Two spatial coexistence mechanisms —— Janzen–Connell (JC) effects and habitat partitioning (HP) —— are frequently invoked to explain high tree diversity in tropical forests (Fig. 1A). JC-effects occur when host-specific enemies reduce juvenile survival near conspecific adults, causing survival to decline with increasing conspecific density. This density-dependent mortality generates negative frequency dependence: rare species gain a per-capita advantage because their enemies are also rare. JC-effects have been documented in forests worldwide (e.g. Hyatt *et al.*, 2003; Mangan *et al.*, 2010; Comita *et al.*, 2014; Song *et al.*, 2021; Hülsmann *et al.*, 2024). By contrast, habitat partitioning occurs when species differ in their responses to the abiotic environment (e.g. topography, soil), such that each species performs best in a subset of habitats (Chesson, 2000a; Snyder & Chesson, 2003; Stein *et al.*, 2014). Many studies — typically measuring the effects of conspecific density and habitat conditions on seedling and sapling survival — find both processes occur simultaneously (e.g. Uriarte *et al.*, 2004; Freckleton & Lewis, 2006; Queenborough *et al.*, 2009; Bai *et al.*, 2012; Piao *et al.*, 2013; Lu *et al.*, 2015; Wu *et al.*, 2016; Johnson *et al.*, 2017; Pu *et al.*, 2017; Cao *et al.*, 2018; Yao *et al.*, 2020; Magee *et al.*, 2021; Huang *et al.*, 2022). It is therefore important to elucidate how they interact.

Although both coexistence mechanisms ultimately maintain diversity by concentrating intraspecific competition relative to interspecific competition (Chesson, 2000b), they shape spatial distributions in opposite ways: habitat partitioning aggregates species in favorable environments (e.g. Andersen *et al.*, 2010; Jones *et al.*, 2011; Brown *et al.*, 2013; John *et al.*, 2007; Potts *et al.*, 2002; Umarani *et al.*, 2024), whereas JC-effects generate conspecific re-

pulsion and overdispersion of adults (Fig. 1D, ii; Chave *et al.*, 2002; Wiegand & Moloney, 2013; Kalyuzhny *et al.*, 2023). Because these mechanisms push spatial patterns in opposite directions, their joint operation may yield non-additive interactions that affect species coexistence in counter-intuitive ways.

Empirical studies account for this tension. Tree species are almost universally aggregated in tropical forests (Condit *et al.*, 2000), a pattern driven by both habitat specialization and dispersal limitation (Baldeck *et al.*, 2013). These aggregation-generating processes complicate empirical detection of negative density dependence: the positive effects of favorable habitats can mask or counteract mortality generated from JC-effects (Wright, 2002; Chen *et al.*, 2010; Bagchi *et al.*, 2011; Wu *et al.*, 2016; Liu *et al.*, 2022; Feng *et al.*, 2023). Dispersal limitation adds further aggregation that is independent of habitat heterogeneity. As a result, spatial point-pattern analyses must disentangle overlapping influences of dispersal, habitat filtering, and density-dependent mortality (Detto & Muller-Landau, 2013; Zhu *et al.*, 2013). Recent analyses at the Barro Colorado Island (BCI) forest dynamics plot illustrate this challenge: strong conspecific repulsion becomes evident only after controlling for aggregation caused by dispersal limitation (Kalyuzhny *et al.*, 2023).

Despite empirical advances in isolating the signal of negative density dependence from dispersal limitation and habitat specialization, theory has not clarified how their joint operation —— and the aggregation patterns they produce — shape species coexistence. Conspecific aggregation can either promote or hinder species richness, depending on the context (Chesson & Neuhauser, 2002; Murrell *et al.*, 2002; Bolker *et al.*, 2003). For example, aggregation can either reduce or enhance coexistence driven by density-dependent processes depending on whether rare species are more or less aggregated than common species (Stump & Comita, 2020; Wiegand *et al.*, 2025). Aggregation driven by dispersal also often positively influences the ability of habitat partitioning to maintain coexistence (Snyder, 2008; D'Andrea & O'Dwyer, 2021). Although both dispersal limitation and habitat specialization generate aggregation, they do so through distinct pathways: dispersal limitation produces clustering

largely independent of habitat heterogeneity, whereas habitat specialization concentrates individuals in locations where they experience high fitness. Because JC-effects modify local environments, these contrasting forms of aggregation may interact with them in different ways (at least when habitats are positively spatially autocorrelated; Fig. 1C vs. Fig. 1D, sub-panel iii). Yet this possibility has received little theoretical attention. The key question is: How do these different forms of aggregation interact with the repulsion generated by JC-effects to shape species coexistence?

Ultimately, the crucial issue is whether interactions between JC-effects and habitat partitioning act synergistically or antagonistically — especially given that past work casts doubt on whether either mechanism alone can explain the extraordinary diversity of tropical forests. Previous theory suggests that while JC-effects can maintain high diversity in otherwise neutral communities (Levi *et al.*, 2019), they are likely insufficient if species differ in fitness. For example, Chisholm & Fung (2020) show that adding realistic interspecific variation in fecundity or low-density recruitment erodes the ability of JC-effects to maintain diversity. Similarly, although habitat partitioning shapes species' spatial distributions and demography, it may not generate enough niches to account for species-rich forest communities. Classical theory holds that the number of coexisting species cannot exceed the number of limiting factors (Levin, 1970; Armstrong & McGehee, 1980); the low dimensionality of abiotic variation relative to the number of species in tropical forests makes habitat partitioning alone unlikely to explain observed diversity (Wright, 2002; Silvertown, 2004; Terborgh, 2015). This raises a central question: Do JC-effects and habitat partitioning, acting together, maintain more or less diversity than the sum of their individual contributions? And how does dispersal limitation modify this interaction? Synergistic interactions would provide a novel explanation for the maintenance of coexistence, whereas antagonistic interactions would deepen the mystery of what sustains diversity. These possibilities likely hinge on the spatial structure of populations. Because density-dependent processes such as JC-effects are inherently non-linear (Detto *et al.*, 2019), their overall contribution to coexistence depends on how individuals are

distributed in space. Aggregation modifies outcomes via non-linear averaging (i.e. Jensen's inequality; Jensen, 1906), such that habitat specialization and dispersal limitation may amplify or dampen both the local strength of density dependence (Chen *et al.*, 2010; Fortunel *et al.*, 2018) and its downstream community-wide consequences.

I analyze a spatially explicit model that incorporates JC-effects, habitat partitioning, and dispersal limitation. I evaluate the ability of each mechanism, alone and in combination, to maintain species richness, with particular attention to how dispersal- versus habitat-driven aggregation modify the contribution of JC-effects to coexistence. The model shows that aggregation from dispersal limitation weakens the ability of JC-effects to maintain diversity. In contrast, aggregation driven by habitat specialization acts synergistically with JC-effects to promote coexistence, often far exceeding the sum of their individual effects. This synergy is captured by the spatial covariance between JC-effects and habitat partitioning ("the JC–HP covariance"): species richness peaks when trees disproportionately generate JC-effects in the environments where they also perform best. Because this covariance can be quantified from spatial data, it provides an empirically grounded metric anchored in coexistence theory establishing a link between tree spatial patterns and the processes that maintain tropical forest diversity.

Methods

Model description

I use a discrete-time site occupancy model similar to those developed by Levi *et al.* (2019), Chisholm & Fung (2020), and Smith (2022). The model tracks the dynamics of a local forest community composed of P patches, each occupied by a single adult tree. The local community contains N species, which draw from a regional pool of R species. Each time step proceeds through four stages: (1) Adults disperse propagules (i.e., seeds) throughout the landscape. (2) Propagules experience mortality due to habitat effects and JC-effects. (3)

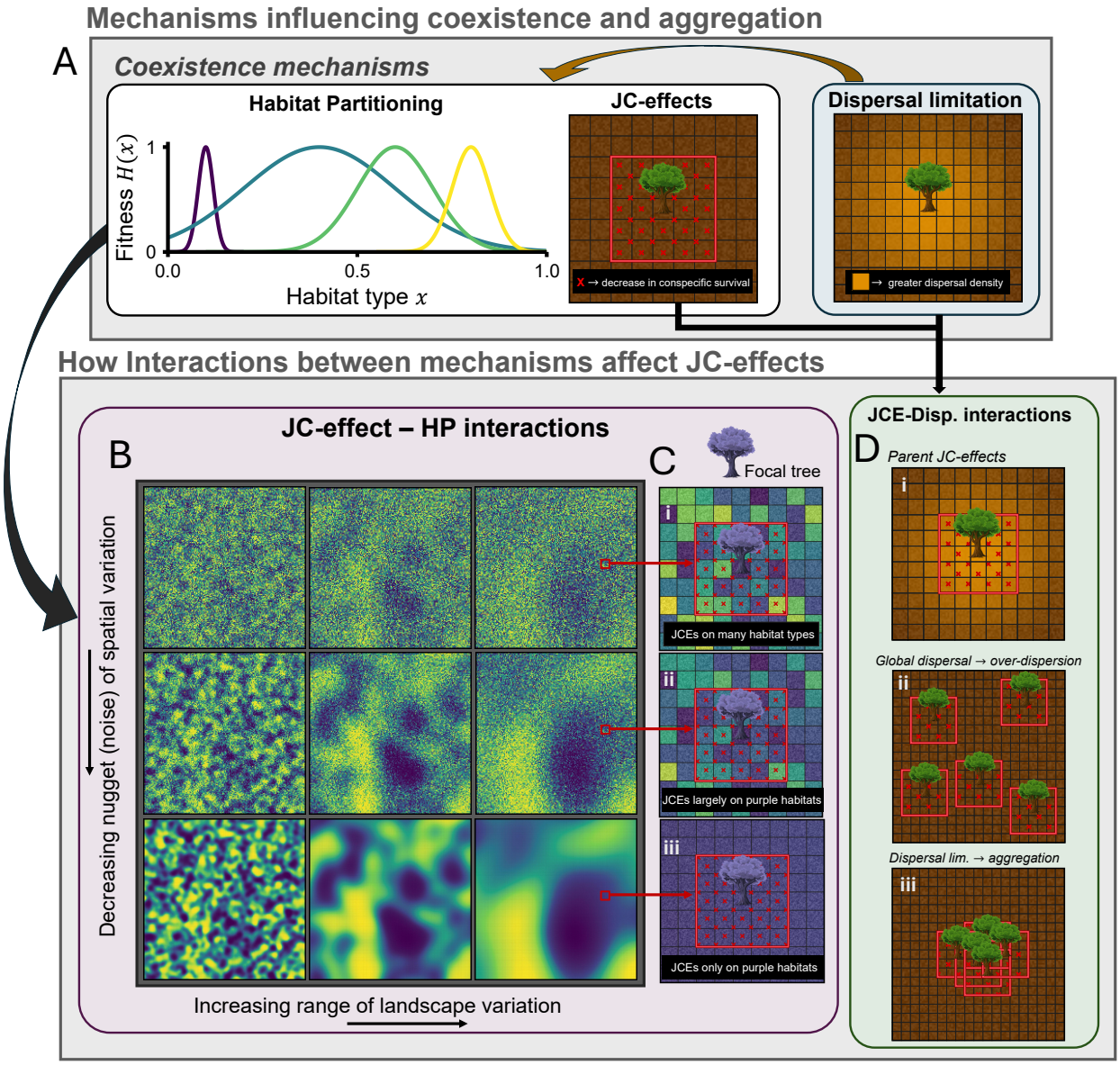

Figure 1: **Conceptual overview of coexistence mechanisms and their interactions.** (A) "Habitat partitioning" shows species responses to the environment $H(x)$ ($\sigma_h = 0.02, 0.2, 0.1$, and 0.05, left to right). "JC-effects" depict the $M \times M$ Moore neighborhood of influence (red) around a focal tree, $M = 5$. "Dispersal limitation" shows the relative propagule pressure from a focal tree (orange shading). (B) Spatial distributions of habitat under varying nugget and range parameters. The nugget controls fine-scale heterogeneity; the range controls the size of habitat patches. Nugget values are 10, 1, and 0 (top to bottom) and range values are 0.05, 0.2, 0.5 (left to right). (C) depicts JC–HP interactions: for a focal tree positively associated with purple habitat patches, the nugget affects which patch types it induces JC-effects on (i-iii). (D) JC-effects interact with dispersal. (i) Locally dispersed propagules are subject to its parent's JC-effects. (ii) Under global dispersal, JC-effects generate overdispersion. (iii) With dispersal limitation, conspecifics may aggregate.

Each adult dies with probability δ. (4) Vacant patches are recolonized either by a propagule from the local seed rain or by an immigrant drawn from the regional species pool.

To model propagule arrival, let x denote a patch (i.e., a discrete grid cell) in space. At each time step, species i ($i = 1, 2, \ldots, N$) disperses propagules across the landscape in proportion to its intrinsic fitness parameter Y_i. This parameter scales the number of propagules contributed by the species and reflects underlying demographic traits such as fecundity, baseline density-independent offspring survival, and competitive ability. Dispersal occurs either globally, with propagules distributed uniformly across all patches, or locally according to a Gaussian kernel with standard deviation σ_D (in grid-cell units), which determines the spatial scale of dispersal. The expected propagule density of species i arriving at patch x is denoted $d_i(x)$. Full details of the dispersal kernel are provided in the Supplementary Information (see "General model derivation and details").

Once propagules arrive, their survival depends on two factors: abiotic habitat effects and JC-effects. I begin by describing habitat effects. Each patch $x \in [0, 1]$ is assigned a habitat value that influences species' demographic performance. The survival of species i's seedlings on patch x is given by a Gaussian response function:

$$H_i(x) = \exp\left(-\frac{(x - h_{\mathrm{opt},i})^2}{2\sigma_h^2}\right). \tag{1}$$

Here, $h_{\mathrm{opt},i}$ is species i's habitat optimum ($0 \leq h_{\mathrm{opt},i} \leq 1$), and σ_h determines niche breadth; smaller σ_h indicates greater specialization. The function $H_i(x)$ ranges between 0 and 1 and captures the relative survival probability of propagules across the habitat axis.

In the main text, I examine the above Gaussian habitat response, in which all species share the same value of σ_h. However, species may also display specialist–generalist trade-offs and exhibit non-Gaussian environmental responses. To test if results were robust to this possibility, I also performed analyses based on the so-called "stress–tolerance–fecundity trade-off" (Muller-Landau, 2010; D'Andrea *et al.*, 2013; D'Andrea & O'Dwyer, 2021), in

which seed size mediates a trade-off between fecundity and tolerance of stressful environments (e.g., drought or low resource availability; Moles *et al.*, 2003; Moles & Westoby, 2004). The stress–tolerance–fecundity trade-off model and related results are described in the Supplementary Information ("Tolerance–fecundity trade-off model"). The key results from the main text are robust to this alternative formulation.

In addition to habitat effects, propagule survival is reduced by JC-effects. These capture mortality imposed by nearby conspecific adults, such as from host-specific pathogens or natural enemies. JC-effects act within an $M \times M$ Moore neighborhood around each patch x, which includes the focal patch and its surrounding neighbors (including diagonals; Fig. 1A). Let $A_i(M(x))$ denote the number of conspecific adults of species i within this neighborhood. The probability that propagules of species i on patch x die due to JC-effects is given by

$$J_i(x) = 1 - \exp\big(- a_i A_i(M(x))\big), \tag{2}$$

where a_i is the baseline strength of JC-effects. Thus, I do not model natural enemies directly. The total JC-effect pressure induced by a single adult of species i is therefore $a_i M^2$ (baseline strength $\times$ spatial scale). The term $1 - e^{-a_i}$ corresponds to the mortality rate experienced when a single conspecific adult is present ($A_i = 1$). Larger values of A_i or stronger baseline sensitivity a_i increase the probability of mortality, while the complementary term $1 - J_i(x)$ gives the probability of surviving JC-effects. This exponential form provides a minimal but biologically reasonable representation of distance- and density-dependent mortality (see Supplementary information "General model derivation and details").

Combining dispersal, habitat effects, and JC-effects, the expected number of viable propagules of species i on patch x is

$$S_i(x) = d_i(x) Y_i H_i(x)\big(1 - J_i(x)\big) \tag{3}$$

where survival after JC-effects is represented by $1 - J_i(x)$. Thus, a species' recruitment on

a patch depends on its dispersal pressure ($d_i(x)$), its intrinsic fitness Y_i, habitat suitability $H_i(x)$, and its probability of surviving JC-effects $1 - J_i(x)$.

Following propagule survival, adult dynamics proceed in three steps. First, at each time step every adult dies with probability δ. Second, if a patch becomes vacant, it is recolonized either from local propagules or by an immigrant drawn from the species in the regional pool. Local recolonization occurs with probability $1-\nu$, while immigration occurs with probability ν. Third, when local lottery competition occurs, species i claims patch x with probability

$$\text{P(species } i \text{ colonizes patch } x) = \frac{S_i(x)}{\sum_{j=1}^{N} S_j(x)}$$

where $S_i(x)$ is the number of surviving propagules from Equation (3). Immigration ensures that the local community reaches a dynamic equilibrium.

Parameterizations for simulations

I used empirical data — largely from the 50-ha Forest Dynamics Plot at BCI — to roughly parameterize key quantities within a biologically feasible range

The spatial scale of JC-effects M strongly influences their ability to maintain species richness (Smith, 2022). In the model, M is the side length (in patches) of the Moore neighborhood within which conspecific adults reduce offspring survival. Its value is determined by two biological quantities: (1) the radius r (in meters) over which JC-effects operate, and (2) the density of reproductive adults per square meter, g. Field studies indicate JC-effects typically decline rapidly beyond 10–20 m from conspecific adults (Hubbell *et al.*, 2001; Johnson *et al.*, 2014), though Kalyuzhny *et al.* (2023) report effects extending further. I assume a more modest JC-effect radius of $r \sim$ 5–15 m. To connect r to M, it is necessary to define how many trees typically fall within r. At BCI, Comita *et al.* (2007) reported approximately 30,000 reproductive adult trees. Other estimates vary depending on the cutoff for reproductive maturity: assuming a 5 cm dbh threshold yields $\sim$ 50,000 woody plant adults (D'Andrea

& O'Dwyer, 2021), while species-specific thresholds yield $\sim$ 80,000 (Chisholm & Fung, 2020). Given that the BCI plot spans 50 hectares (5×10^5 m^2), these values imply adult densities of $g \sim 0.06$–0.10 individuals per m^2. In the model's square-lattice geometry, neighboring patches are separated by $1/\sqrt{g}$ m (i.e., each patch has area $1/g$ m^2 and each side length is $1/\sqrt{g}$ m). $M/2$ can be interpreted as the number of patch-lengths spanning the JC-effect radius and thus a Moore neighborhood of size M covers a spatial radius of $(M/2)(1/\sqrt{g})$ m. Rearranging gives $M = 2r\sqrt{g}$. Using the empirical ranges of r and g yields approximate values of M between 3 and 9. Slightly more conservatively, I ran simulations using $M \in 1, 3, 5, 7$, spanning small-scale to relatively large neighborhood effects.

The baseline strength of JC-effects, a, also plays a central role in determining species richness (Smith, 2022). Meta-analyses suggest that seedling survival near a conspecific adult is reduced by roughly 60%, which corresponds to $a \approx 1$ under the exponential mortality function (Comita *et al.*, 2014; Song *et al.*, 2021). For most simulations, I adopted a more conservative baseline value of $a = 0.5$. Unless otherwise noted, species were assumed to share the same baseline JC-effect strength. Because empirical studies also document substantial interspecific variation in sensitivity to conspecific density (Comita *et al.*, 2010; Song *et al.*, 2021), I additionally ran simulations in which a varied among species, with values drawn from a gamma distribution (see Supplementary Information "Interspecific variation in baseline JC-effect strength). Adding interspecific variation in a did not qualitatively change results.

Substantial interspecific variation in fitness-related demographic rates (e.g., fecundity, density-independent survival, and growth) is well documented in tropical forests such as BCI. In particular, fecundity and related rates often exhibit fat-tailed distributions (Dalling *et al.*, 2002; Wright *et al.*, 2005; Chisholm & Fung, 2020). Following Chisholm & Fung (2020) and D'Andrea & O'Dwyer (2021), I represent intrinsic fitness (Y) as a log-normally distributed variable: $Y \sim \text{lognormal}(\mu = 0, \sigma_Y)$. Y captures multiple life-history traits and demographic rates, including fecundity, density-independent juvenile survival, seedling growth, and general competitive ability. For most simulations, I adopt a value of $\sigma_Y = 0.3$,

which produces roughly an order of magnitude of variation in fitness among species — sufficient to test the robustness of coexistence mechanisms.

Species' responses to abiotic heterogeneity — quantified by the niche-breadth parameter σ_h — are difficult to estimate directly because they integrate over multiple environmental factors that are rarely directly measured for most tropical tree species. I therefore explored a broad range of σ_h values in simulations, spanning from $\sigma_h = 0.02$ to $\sigma_h = 0.2$. Lower values (e.g., $\sigma_h = 0.02$; Fig. 1A, blue curve) represent relatively specialized species, while higher values (e.g., $\sigma_h = 0.2$; Fig. 1A, red curve) represent generalized responses. In simulations, each species' habitat optimum, $h_{\mathrm{opt},i}$, was drawn uniformly on $[0, 1]$. As noted earlier, I also considered an alternative formulation in which species experience a stress–tolerance–fecundity trade-off to test robustness (Supplementary Information).

I explored a range of dispersal limitation values, characterized by the dispersal kernel standard deviation σ_D, from highly limited local dispersal ($\sigma_D = 1$) to global dispersal ($\sigma_D = \infty$). For simplicity, all species were assumed to share the same value of σ_D.

I used a low immigration rate of $\nu = 0.3 \times 10^{-5}$, which yields $\sim$ 1–3 species at equilibrium in a neutral community. This ensures that effectively all species richness in simulated communities can be attributed to JC-effects, habitat partitioning, or their interaction.

Simulations were run on a 175×175 grid, yielding $\sim$ 30,000 patches, each occupied by a single adult tree — comparable to the number of reproductive adults at BCI. Each patch was assigned a habitat value between 0 and 1. To investigate the effects of habitat-driven aggregation, I generated spatial habitat landscapes as Gaussian random fields using the Julia package GaussianRandomFields (Robbe, 2023), and rescaled values to a uniform $[0, 1]$ distribution (preserving spatial ranks). These fields are parameterized by three quantities: the sill, the range, and the nugget. The sill sets the total variance of the field at large distances (fixed at 1 here for convenience), while the range specifies the distance at which sites become effectively uncorrelated (Fig. 1B, left to right) — formally, the range is the point where the variogram rises to 95% of the sill (Cressie, 1993; D'Andrea & O'Dwyer, 2021). With the

parameterizations used here, a range of e.g. 0.5 implies the variogram reaches 95% of the sill at a distance of 50% of the total landscape side length. The nugget adds microscale white-noise variance to each point, producing local roughness without altering large-scale patchiness (Fig. 1B, top to bottom). Overall, the range controls the size of habitat patches, while the nugget controls their fine-scale heterogeneity.

Aggregation metrics

In several parts of the analysis, I quantify species aggregation using two complementary metrics. First, as a simple measure of intraspecific spatial aggregation of adult trees in simulations, I computed $\kappa_{i,M} = \frac{\sigma^2_{i,M}}{\mu_{i,M}}$ where $\mu_{i,M}$ and $\sigma^2_{i,M}$ are the mean and variance of species i's abundance across all $M \times M$ Moore neighborhoods. Here $\mu_{i,M} = p_i M^2$, with p_i the proportion of patches occupied by species i. This local variance–to–mean ratio satisfies $\kappa_{i,M} = 1$ under spatial randomness, $\kappa_{i,M} > 1$ under aggregation, and $\kappa_{i,M} < 1$ under regular spacing. As a community-level summary, I use the average

$$\overline{\kappa}_M = \frac{1}{N} \sum_{k=1}^{N} \kappa_{k,M}. \tag{4}$$

Because the scale M matches the neighborhood scale of JC-effects, this metric quantities the outcome of interactions between the aggregation-generating processes (habitat partitioning and dispersal limitation) and the local repulsion imposed by JC-effects.

Second, I consider the pair-correlation function, which is the scale–specific counterpart of Ripley's K–function (Ripley, 1976) and commonly used in spatial point pattern analyses (Wiegand & Moloney, 2013). For a point process of constant intensity λ, the K-function is defined so that, for a typical individual (of a focal species), the expected number of other individuals within distance r is $\lambda K(r)$. Under complete spatial randomness (CSR), $K(r) = \pi r^2$, while values above or below this benchmark indicate aggregation or inhibition, respectively. The pair-correlation function $g(r)$ is obtained from $K(r)$ as $g(r) = \frac{K'(r)}{2\pi r}$, so that

$g(r)$ measures the relative density of pairs of individuals separated by distance r, normalized against CSR. By definition, $g(r) = 1$ under CSR, values $g(r) > 1$ indicate aggregation, and values $g(r) < 1$ indicate overdispersion (regular spacing). In analyzing the simulations, I treat each individual as located at the center of its occupied grid cell, so that the community can be regarded as a point pattern in continuous space with unit cell spacing. Analysis of $g(r)$ allows quantification of aggregation at multiple spatial scales.

Analysis and simulations

I combined mathematical analyses with simulations of the spatially explicit model. First, I derived an approximate analytical condition under which a rare species deterministically increases in abundance when introduced into a community of N resident species in the local community. This was accomplished by deriving when the quantity $\tilde{\lambda}_i = (\lambda_i - 1)/\delta > 0$ as $p_i \to 0$ where $\lambda_i = \frac{p_i(t+1)}{p_i(t)}$ is the finite rate of increase and δ is the adult mortality rate. I refer to $\tilde{\lambda}_i$ as the weighted growth rate of species i (Chesson, 2003). See Supplementary Information "Invasion criteria" for a detailed derivation.

Next, I conducted forward-in-time simulations on the 175×175 grid, on a torus to eliminate edge effects. The local community was initialized with species drawn from the regional pool. In most simulations, I assumed the regional pool contained 500 species, although I also tested how the regional pool size affects local community species richness. Simulations were run for $\sim$ 10,000 generations — sufficient for species richness to reach a dynamic equilibrium maintained by the balance of extinction and immigration.

With these specifications, I conducted four main sets of simulations. **(1) Regional pool size and local species richness.** I performed simulations varying the regional pool size under five different scenarios: when only JC-effects occur, when only habitat partitioning occurs, and when both occur under low, intermediate, and high levels of spatial autocorrelation (defined by the nugget). **(2) Mechanism synergy analysis.** Using the parameterizations described in above section, I examined the *synergy* of JC-effect – habitat partitioning inter-

actions. I defined the *synergy* of JC-effects and habitat partitioning as the factor by which species richness under their joint operation exceeds the sum of their separate contributions. For example, with $M = 7$ and $\sigma_h = 0.02$, letting "SR" denote species richness:

$$\text{Synergy} = \frac{\text{SR}(M = 7,\ \sigma_h = 0.02)}{\text{SR}(M = 7,\ \text{no HP}) + \text{SR}(\sigma_h = 0.02,\ \text{no JCEs})}. \tag{5}$$

I refer to JC-effect–habitat partitioning interactions with synergy > 1 as "synergistic" and those with < 1 as "antagonistic." **(3) Drivers of aggregation and coexistence.** I investigated how processes shaping species' spatial distributions — dispersal limitation (σ_h), JC-effect strength (a), and spatial autocorrelation (quantified by the nugget) — combine to influence the relationship between aggregation and species richness. **(4) The spatial scale of JC-effects.** I examined how the spatial scale of JC-effects *per se* influences species richness. The overall strength of JC-effects depends on both their baseline intensity (a) and their spatial extent (M^2), such that the total intensity generated by an individual tree is aM^2. To isolate the role of JC-effect spatial scale, I ran simulations varying M while holding $aM^2 = K$ constant. I then compared how species richness responds to spatial scale when (1) only JC-effects operate (with and without dispersal limitation) and (2) when both JC-effects and habitat partitioning are present.

All simulations were implemented in Julia version 1.11 (Bezanson *et al.*, 2017). Figures were produced in R version 4.3.2 (R Core Team, 2021).

Results

Invasion criteria

This invasion analysis has two aims. First, to examine how the contributions to coexistence of JC-effects, habitat partitioning, and their interaction scale with N, the number of resident species in the local community. This allows an understanding their ability to maintain

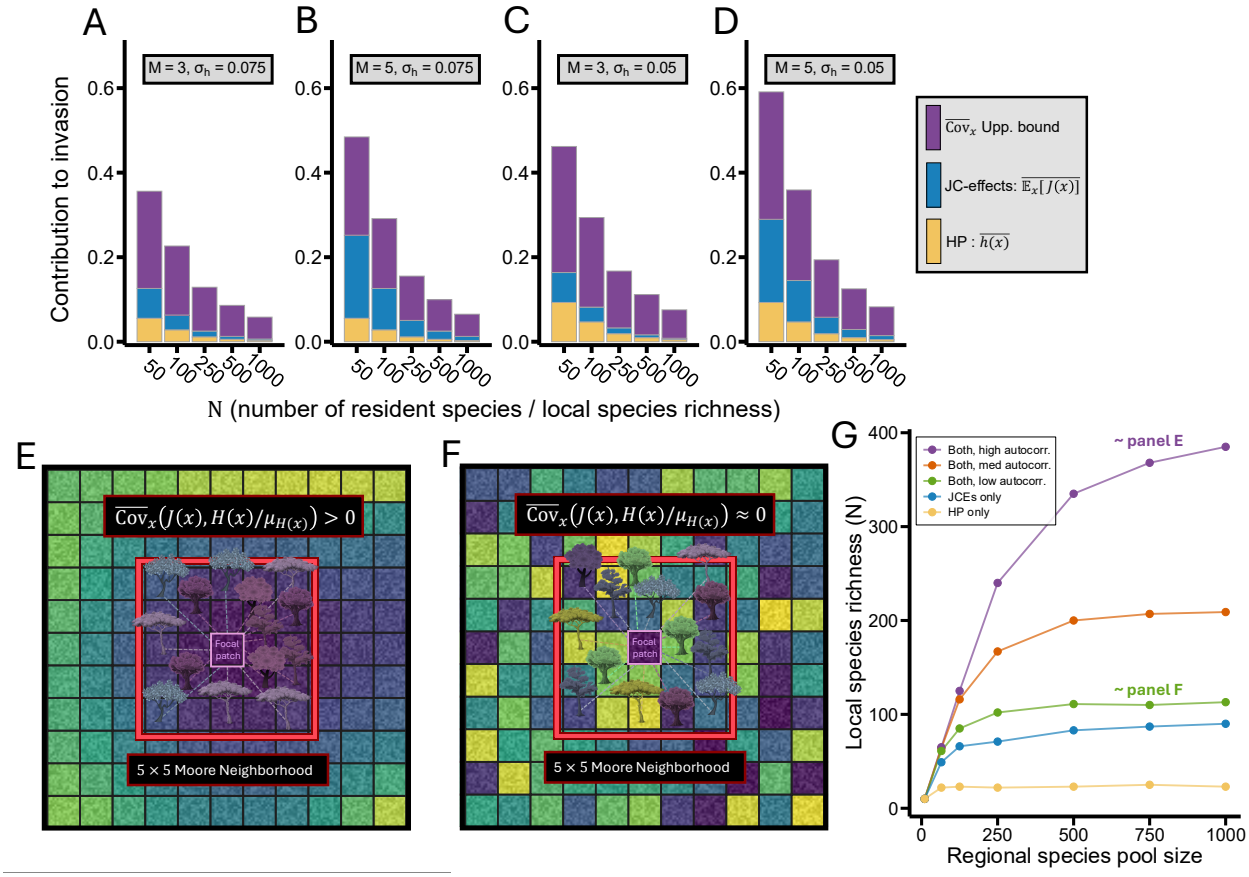

Figure 2: **The JC–HP covariance can generate substantial stabilization in highly diverse communities.** (A-D) Stabilizing contributions due to habitat partitioning (HP; yellow), JC-effects (blue), and the upper bound of the JC–HP covariance (purple) as a function of resident species richness (N). All plots use $a = 0.5$. (E) and (F) Illustrate JC–HP covariance when habitats are highly vs. lowly spatially autocorrelated, respectively. Color indexes tree preference. (G) Simulations. The x-axis shows the number of species in the regional pool, and the y-axis shows local species richness at equilibrium N. Colored curves correspond to five scenarios labeled in the legend. In all simulations, $\sigma_D = \infty$, $a = 0.5$, $\nu = .3 \times 10^{-5}$, $Y \sim \text{lognormal}(\mu = 0, \sigma_Y = 0.3)$, $M = 7$ (except HP only), $\sigma_h = 0.02$ (except JCEs only), and habitat range $= 0.5$. Low, medium, and high autocorrelation are defined by nugget $= 10$ (similar to panel F), 0.1, or 0 (similar to panel E), respectively.

coexistence in highly diverse communities. Second, to distinguish the effects on coexistence of aggregation arising from dispersal limitation versus habitat specialization. To this end, I consider two cases: (1) JC-effects with habitat partitioning under global dispersal, and (2) JC-effects alone with dispersal limitation. Although dispersal also interacts with habitat partitioning, these two cases capture the essential contrasts while keeping the analysis tractable.

JC-effects, habitat partitioning, and global dispersal

Suppose species i is a rare invader with intrinsic fitness Y_i, habitat optimum $h_{\mathrm{opt},i}$, and assume dispersal is global. Let $\overline{H_i(x)} = \mu_{H_i(x)}$ denote the mean performance of species i across space x. Then species i invades if its weighted growth rate is positive:

$$\tilde{\lambda}_i \approx \underbrace{\ln Y_i - \overline{\ln Y}}_{\text{Fitness differences}} + \underbrace{\overline{\mathbb{E}_x[J(x)]}}_{\text{JC-effects}} + \underbrace{\overline{h(x)}}_{\text{Habitat effects}} + \underbrace{\overline{\mathrm{Cov}_x}\left(J(x), \frac{H(x)}{\mu_{H(x)}}\right)}_{\text{JC–HP covariance}} > 0 \tag{6}$$

See Supplementary Information ("JC-effects and habitat partitioning, no dispersal limitation") for the derivation. Note that this invasion criterion is quite general and flexible to different functional forms of $J(x)$ and $H(x)$. Below I emphasize the functional forms presented in the Methods section, and assume species have identical breadths, $\mu_{H_i(x)} = \mu_{H_k(x)} = \mu_{H(x)}$ ($k = 1, 2, \ldots, N$), for analytical tractability. $\tilde{\lambda}_i$ consists of four terms: a fitness-difference term and three stabilizing mechanisms (Chesson, 2000b). I discuss these in detail below.

First, $\overline{\ln Y} = \frac{1}{N}\sum \ln Y_k$ is the mean log fitness of the resident species. Thus, $\ln Y_i - \overline{\ln Y}$ represents the invader's fitness difference relative to the mean resident fitness. If this difference is negative, the stabilizing mechanisms must be sufficiently strong to permit invasion.

Second, the direct contribution of JC-effects, $\overline{\mathbb{E}_x[J(x)]}$, is the mean JC-effect strength across space x, averaged over resident species: $\overline{\mathbb{E}_x[J(x)]} = \frac{1}{N}\sum_{k=1}^{N} \mathbb{E}_x[J_k(x)]$. Using the

form in equation 2, this yields

$$\overline{\mathbb{E}_x[J(x)]} \approx (1 - e^{-a})\frac{M^2}{N}, \tag{7}$$

where a is the baseline JC-effect strength, M is the spatial scale, and N is the number of resident species. This approximation assumes adults are randomly distributed in space. Intuitively, stronger baseline JC-effects (a) and larger neighborhoods (M) promote coexistence. However, because $\overline{\mathbb{E}_x[J(x)]}$ decreases in proportion to $1/N$, the ability of JC-effects to maintain coexistence declines rapidly as species richness increases (Fig. 2A, blue bars).

Aggregation reduces $\overline{\mathbb{E}_x[J(x)]}$. To see this, I derived an alternative approximation that relaxes the assumption of spatial randomness:

$$\overline{\mathbb{E}_x[J(x)]} \;\approx\; \frac{aM^2}{N}\left(1 - \frac{a}{2}\,\overline{\kappa}_M\right), \tag{8}$$

where $\overline{\kappa}_M$ is the mean intraspecific aggregation of residents at the $M \times M$ scale (equation 4). This approximation is valid when a and $\overline{\kappa}_M$ are not too large (i.e., the expression remains non-negative within the parameter space where the approximation applies). Thus, aggregation *per se* reduces the ability of JC-effects to stabilize coexistence (see Supplementary Information, "Moment-based approximation of $\overline{\mathbb{E}_x[J(x)]}$," for details).

Third, the "Habitat effects" term $\overline{h(x)}$ captures the contribution to invasion that arises from differences in species' responses to the environment. A full derivation is given in the Supplementary Information ("Derivation of $\overline{h(x)}$"), but the structure is particularly transparent when all species (including the invader) have the same average correlation in their habitat responses. In this case

$$\overline{h(x)} = \frac{1}{N}\,\mathrm{CV}^2_{H(x)}\,(1 - \bar{r}), \tag{9}$$

where $\mathrm{CV}^2_{H(x)} = \sigma^2_{H(x)}/\mu^2_{H(x)}$ is the squared coefficient of variation of habitat responses, and

$\bar{r}$ is the average correlation in habitat responses across species. Intuitively, stabilization is strongest when responses are weakly correlated ($\bar{r} \to 0$), and it vanishes as responses become more tightly aligned ($\bar{r} \to 1$).

Using the Gaussian response function from equation (1), one can further obtain a closed-form expression under the assumption of specialized niches ($\mu_{H(x)} \ll 1$). In this regime, $\mu_{H(x)} \approx \sigma_h\sqrt{2\pi}$ and $\mathrm{CV}^2_{H(x)} \approx \frac{1}{\sqrt{2}\,\mu_{H(x)}} - 1$. Substituting into equation (9) and assuming $\bar{r} \simeq 0$ (as expected when habitat optima are randomly distributed) yields

$$\overline{h(x)} \;\approx\; \frac{1}{N}\left(\frac{1}{2\sigma_h\sqrt{\pi}} - 1\right). \tag{10}$$

Thus, narrower niches (smaller σ_h) strengthen stabilization, but—just as with JC-effects—the effect is diluted by community size N (Fig. 2A, yellow bars).

Fourth, the interaction between JC-effects and habitat partitioning (the JC–HP covariance) is given by

$$\overline{\mathrm{Cov}_x}\Big(J(x), \tfrac{H(x)}{\mu_{H(x)}}\Big) = \frac{1}{N}\sum_{k=1}^{N} \mathrm{Cov}_x\Big(J_k(x), \tfrac{H_k(x)}{\mu_{H_k(x)}}\Big), \tag{11}$$

where Cov_x is the spatial covariance between JC-effect strength and habitat effects scaled by specialization. A positive JC–HP covariance promotes invasion. The mechanism reflects a key principle: invaders experience their strongest competition in habitats favorable to them, which are also preferred by resident species with similar optima. If those residents disproportionately generate JC-effects in those same habitats—as occurs under spatial autocorrelation—resident fitness is reduced more strongly than if JC-effects were induced in unfavorable habitats. This yields $\overline{\mathrm{Cov}_x}\big(J(x), H(x)/\mu_{H(x)}\big) > 0$ (Fig. 2E). In contrast, when habitats are randomly distributed, $\overline{\mathrm{Cov}_x}\big(J(x), H(x)/\mu_{H(x)}\big) \approx 0$, and JC-effects and HP do not interact (Fig. 2F).

The JC–HP covariance term can exceed the direct effects of $\overline{\mathbb{E}_x[J(x)]}$ and $\overline{h(x)}$. Using the Cauchy–Schwarz inequality ($\mathrm{Cov}\big(J(x), H(x)\big) \leq \sigma_{J(x)}\sigma_{H(x)}$), I derived two approximate upper bounds. Conceptually, the bound occurs when species' JC-effects are maximally con-

centrated in habitats favorable to them (Fig. 2E; see Supplementary Information, "Upper bound on JC–HP covariance").

First, heuristically,

$$\overline{\mathrm{Cov}_x}\Big(J(x), \tfrac{H(x)}{\mu_{H(x)}}\Big) \lesssim \underbrace{\frac{aM}{\sqrt{N}}\sqrt{\overline{\kappa}_M}}_{\approx\, \sigma_{J(x)}} \quad \times \quad \underbrace{\frac{\sigma_{H(x)}}{\mu_{H(x)}}}_{\text{CV of } H(x)} \quad . \tag{12}$$

Stabilization due to the JC–HP covariance increases with mean intraspecific aggregation $\overline{\kappa}_M$. This contrasts with the direct JC-effect term, which decreases in strength with aggregation (eq. 2). The bound also scales with the coefficient of variation (CV) of habitat responses.

Second, assuming $\mu_{H(x)} \ll 1$ and species are maximally aggregated in space (so that $\sigma_{J(x)}$ attains its upper bound), a tighter approximation is

$$\overline{\mathrm{Cov}_x}\Big(J(x), \tfrac{H(x)}{\mu_{H(x)}}\Big) \lesssim \underbrace{(1-e^{-aM^2})\sqrt{\tfrac{1}{N}\big(1-\tfrac{1}{N}\big)}}_{\approx\, \sigma_{J(x)} \text{ upper bound}} \underbrace{\sqrt{\tfrac{1}{\mu_{H(x)}\sqrt{2}}-1}}_{\approx \text{ CV of } H(x)} . \tag{13}$$

where, as above, $\mu_{H(x)} \approx \sigma_h\sqrt{2\pi}$. For both bounds, the contribution of the JC–HP covariance to invasion is $\propto 1/\sqrt{N}$, which decays more slowly with species richness than the direct effects of JC-effects or habitat partitioning ($\propto 1/N$). Thus, even when the direct effects are weak — such as when N is large — the interaction can provide substantial stabilization (Fig. 2A–D; purple vs. blue and yellow bars). Figure 2 plots this tighter bound.

An additional insight is that the JC–HP covariance does not require interspecific variation in habitat preferences. Indeed, such differences do not appear in the expression. Consider a scenario where (1) all species share the same habitat preference and (2) some patches are uninhabitable for all species. If habitats are uncorrelated, the JC–HP covariance is zero. By contrast, positive spatial autocorrelation causes species to aggregate in favorable patches and disproportionately generate JC-effects there, yielding a positive JC–HP covariance. This occurs because JC-effects in uninhabitable patches have no impact on fitness and thus do

not stabilize coexistence, whereas JC-effects in habitable patches are stabilizing.

JC-effects and dispersal limitation

With local dispersal, propagules deposited near a parent tree are subject to its JC-effects (Fig. 1D, i). Let d denote the proportion of propagules that disperse far enough to avoid JC-effects within the parent's $M \times M$ Moore neighborhood. In this case, invasion occurs when

$$\tilde{\lambda}_i \approx \ln Y_i - \overline{\ln Y} + \overline{\mathbb{E}_x[J(x)]}\Big(d + (1-d)e^{-a}\Big) > 0. \tag{14}$$

See Supplementary Information ("JC-effects, dispersal limitation, and no habitat partitioning") for the derivation. Dispersal limitation reduces the contribution of JC-effects to invasion relative to global dispersal through two mechanisms.

First, the loss of locally dispersed propagules weakens the impact JC-effects have on invasion (see also Stump & Chesson, 2015). The term $\overline{\mathbb{E}_x[J(x)]}$ is multiplied by the factor $d + (1-d)e^{-a} \leq 1$, so stabilization declines as dispersal becomes more limited (smaller d). A fraction $1-d$ of propagules remain near the parent and experience JC-effects, weakening the advantage of rarity.

Second, dispersal limitation leads to intraspecific aggregation (Fig. 1D, iii). As shown in equation 8, aggregation directly reduces $\overline{\mathbb{E}_x[J(x)]}$.

Simulations

JC-effects and habitat partitioning in isolation

Local species richness N maintained by JC-effects alone or habitat partitioning alone saturated rapidly with regional pool size (Fig. 2G, blue and yellow curves).

When only JC-effects operated, the number of coexisting species increased with their spatial scale (M). With $a = 0.5$, up to ∼80–90 species persisted (Fig. 3A–B, "No HP" row, $M = 7$; Fig. 2G). Dispersal limitation ($\sigma_D = 1.5$) reduced richness relative to global

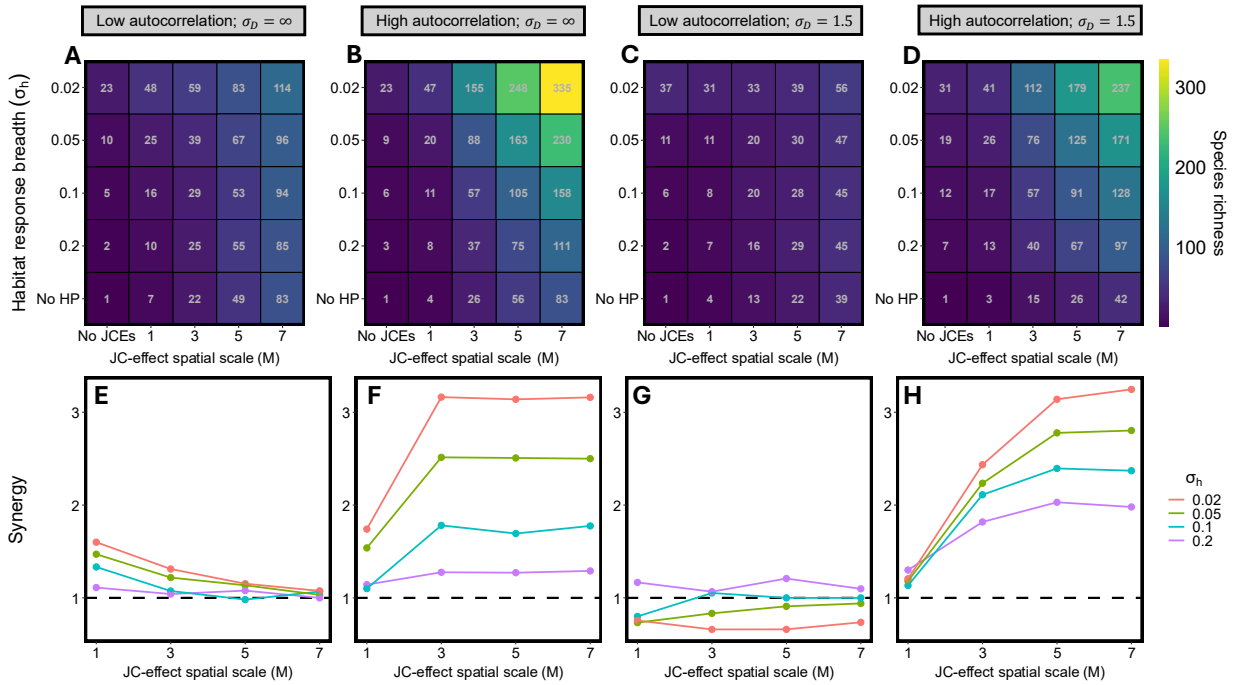

Figure 3: **Spatial autocorrelation and dispersal limitation jointly influence JC–HP synergy.** Each column represents a different case, defined by the level of spatial autocorrelation and dispersal limitation (see panel labels). (A–D) show equilibrium species richness (color scale) across combinations of JC-effect scale (M, x-axis) and niche breadth (σ_h, y-axis). (E–H) show the corresponding synergy for each parameter combination in the above plots. In all simulations, $a = 0.5$, $\nu = 0.3 \times 10^{-5}$, $Y \sim \text{lognormal}(\mu = 0, \sigma_Y = 0.3)$, and the habitat range was set to 0.5. High spatial autocorrelation corresponds to nugget $= 0$, while low autocorrelation corresponds to nugget $= 10$.

dispersal, sometimes by more than 50% (compare Fig. 3A "No HP" row with Fig. 3C).

When only habitat partitioning operated, richness increased with greater specialization (smaller σ_h; Fig. 3, "No JCEs" column). Roughly 20–30 species persisted under narrow niches and global dispersal ($\sigma_h = 0.02$; see Fig. 1A, purple curve, for niche width). Unlike JC-effects, habitat partitioning yielded higher richness under dispersal limitation (compare "No JCEs" columns in Fig. 3A,B vs. C,D), with ∼30–40 species coexisting under the narrowest niches examined (Fig. 3C,D).

These results should be interpreted as a frame of reference: larger a or M^2 and smaller σ_h would all increase species richness. Below, I examine how the joint operation of JC-effects and habitat partitioning differs from the sum of their parts relative to these baseline results.

Joint operation of JC-effects and habitat partitioning

Outcomes depended strongly on the degree of spatial autocorrelation in habitat structure when both mechanisms acted together. Local species richness N saturated quickly at a maximum value as the size of the regional pool increased under low spatial autocorrelation (Fig. 2G, green curve). In contrast, saturation was much slower under moderate or strong autocorrelation (blue and purple curves, respectively). For example, under otherwise identical parameters, highly autocorrelated environments maintained ∼400 species, compared with ∼100 species in weakly autocorrelated environments (Fig. 2G, purple vs. green curves at a regional pool size of 1000). More generally, species richness was higher under high spatial autocorrelation (compare Fig. 3A to 3B and 3C to 3D) and under global dispersal (compare Fig. 3A to 3C and 3B to 3D) when both JC-effects and habitat partitioning operated.

JC–HP interactions ranged from weakly synergistic to antagonistic when spatial autocorrelation was low, but were typically highly synergistic when autocorrelation was high (Fig. 3; see equation 5 for the definition of synergy). Under low autocorrelation and global dispersal ($\sigma_D = \infty$; Fig. 3A,E), JC-effects and habitat partitioning were moderately synergistic when $M = 1$, with synergy up to ≈ 1.5 under narrow niches ($\sigma_h = 0.02$). However, synergy

declined with JC-effect scale M, disappearing by $M = 7$ (Fig. 3E). With dispersal limitation ($\sigma_D = 1.5$; Fig. 3C,G), synergy was largely absent and became antagonistic under narrow niches (small σ_h; Fig. 3G, orange and green curves).

High spatial autocorrelation yielded synergistic interactions in all cases. While large M eliminated synergy under low spatial autocorrelation (Fig. 3E), it amplified synergy under high autocorrelation, with values exceeding 3 (Fig. 3F,H). Moreover, synergy was often greater under dispersal limitation than under global dispersal (compare Fig. 3F to 3H), again in contrast to the low-autocorrelation case, where dispersal limitation led to antagonistic interactions.

The increase in species richness associated with positive spatial autocorrelation is driven by the JC–HP covariance. In simulations varying the range and nugget of spatial variation, species richness closely tracked the JC–HP covariance (compare Fig. 4A,B). Richness increased approximately linearly with the JC–HP covariance term in these simulations (Fig. 4C). This linear association was robust both when species differed in baseline JC-effect strength a (Supplementary Information, "Interspecific variation in baseline JC-effect strength") and when species exhibited a specialist–generalist trade-off in their habitat responses (Supplementary Information, "Tolerance–fecundity trade-off model").

Intraspecific aggregation and species richness

The relationship between species aggregation and species richness differed qualitatively depending on the mechanism generating aggregation. Consider first the case of JC-effects alone. Stabilization increases with the baseline strength a (equations 2 and 8), and correspondingly, species richness increases with a (Fig. 5A). When a is large (e.g., $a > 10$), conspecific recruitment is effectively impossible within the Moore neighborhood. This reduces aggregation and produces regular/overdispersed conspecific spacing (Fig. 5M; $\overline{\kappa}_M < 1$ in Fig. 5E; pair-correlation function $g(r) < 1$ for small r in Fig. 5M). Thus, species richness decreased with increasing aggregation (Fig. 5F). Similarly, dispersal limitation reduced rich-

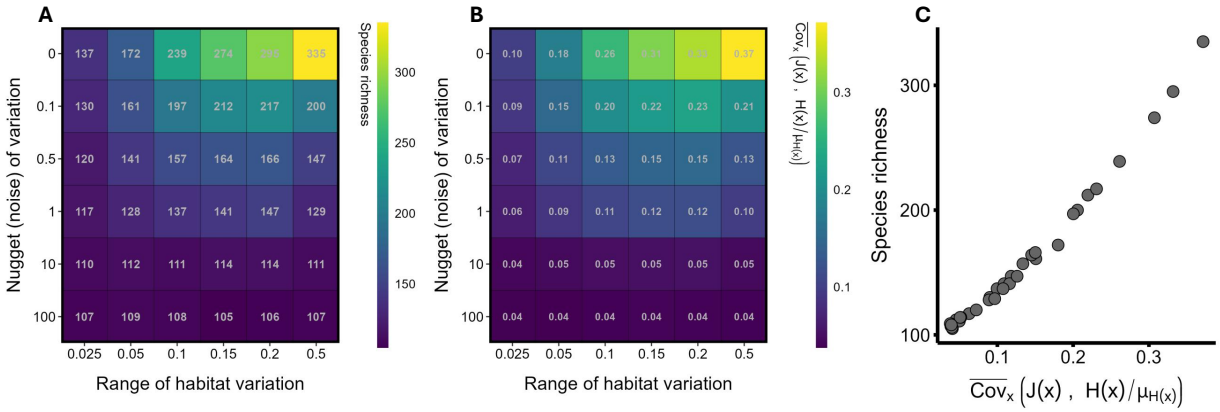

Figure 4: **When both JC-effects and habitat partitioning operate, species richness increases with abiotic habitat spatial autocorrelation, driven by the JC–HP covariance.** All panels depict simulations in which the range and nugget (noise term) of spatial variation were varied. (A) and (B) show how the range and nugget influence species richness and the JC–HP covariance, respectively. (C) shows the relationship between species richness and the JC–HP covariance across simulations. Parameters: $a = 0.5$, $\nu = 0.3 \times 10^{-5}$, $\sigma_h = 0.02$, $Y \sim \text{lognormal}(\mu = 0, \sigma_Y = 0.3)$, $M = 7$, and dispersal is global.

ness, again generating a negative relationship between richness and aggregation (Fig. 5B,F; $g(r) > 1$ for small r in Fig. 5J,N). In sum, under JC-effects alone, aggregation and richness were negatively associated.

In contrast, when both JC-effects and habitat partitioning were present, aggregation driven by habitat specialization was associated with greater species richness. As in Fig. 4, richness increased as the nugget (environmental noise) decreased (Fig. 5C). This produced a positive relationship between richness and aggregation (Fig. 5G): low richness occurred when species exhibited regular spacing ($g(r) < 1$ for small r; Fig. 5O), whereas high richness occurred when species were highly aggregated at small spatial scales ($g(r) > 1$ for small r; Fig. 5P).

The relationship between richness and aggregation in Fig. 5G does not arise from habitat partitioning *per se*. Under global dispersal, aggregation driven by habitat specialization was unrelated to species richness when JC-effects were absent (Fig. 5D,H). Thus, the positive aggregation–richness association stems entirely from how habitat partitioning modifies the operation of JC-effects.

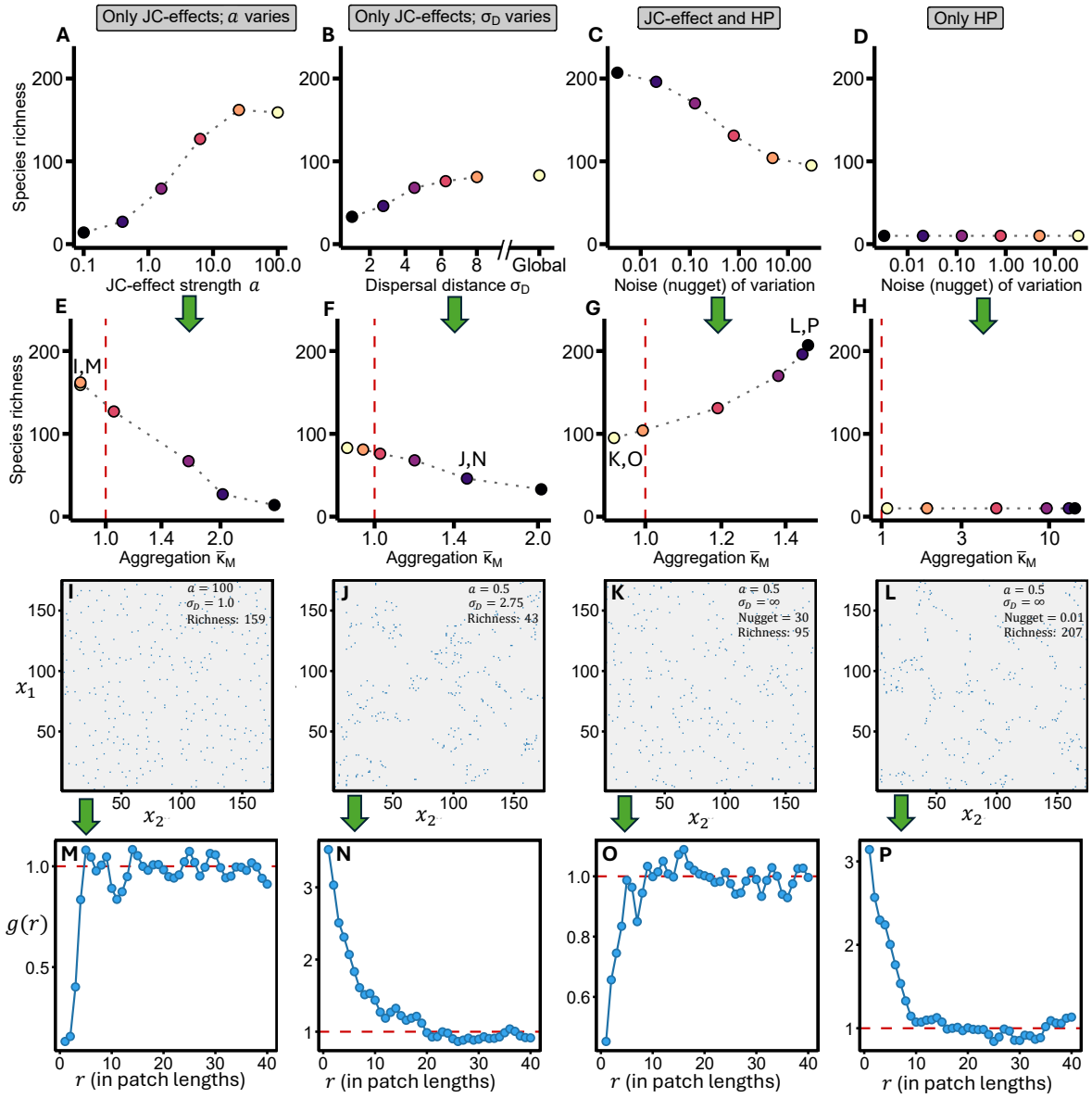

Figure 5: **Aggregation driven by habitat partitioning vs. dispersal limitation has qualitatively different effects on species richness.** (A–D) show species richness as a function of the specified parameters; (E–H) show richness as a function of mean intraspecific aggregation $\overline{\kappa}_M$ in the corresponding simulations (see green arrows). Points of the same color in, e.g., A and E represent the same simulation. (A,E) JC-effects only, varying a; $\sigma_D = 1.0$. (B,F) JC-effects only, varying dispersal limitation σ_D; $a = 0.5$. (C,G) Joint operation of JC-effects and habitat partitioning, varying the nugget of habitat variation; $\sigma_D = \infty$. (D,H) Same parameters as (C,G), but with habitat partitioning only. (I–L) Spatial distribution of one species with an abundance of ∼300 individuals, selected from a labeled simulation in E, F, or G. (M–P) Pair-correlation function $g(r)$ for the focal individual; r indicates the number of patch lengths. All simulations use $\nu = 0.3 \times 10^{-5}$, $Y \sim \text{lognormal}(\mu = 0, \sigma_Y = 0.3)$, $M = 7$, $\sigma_h = 0.05$, and habitat range = 0.5 (when relevant).

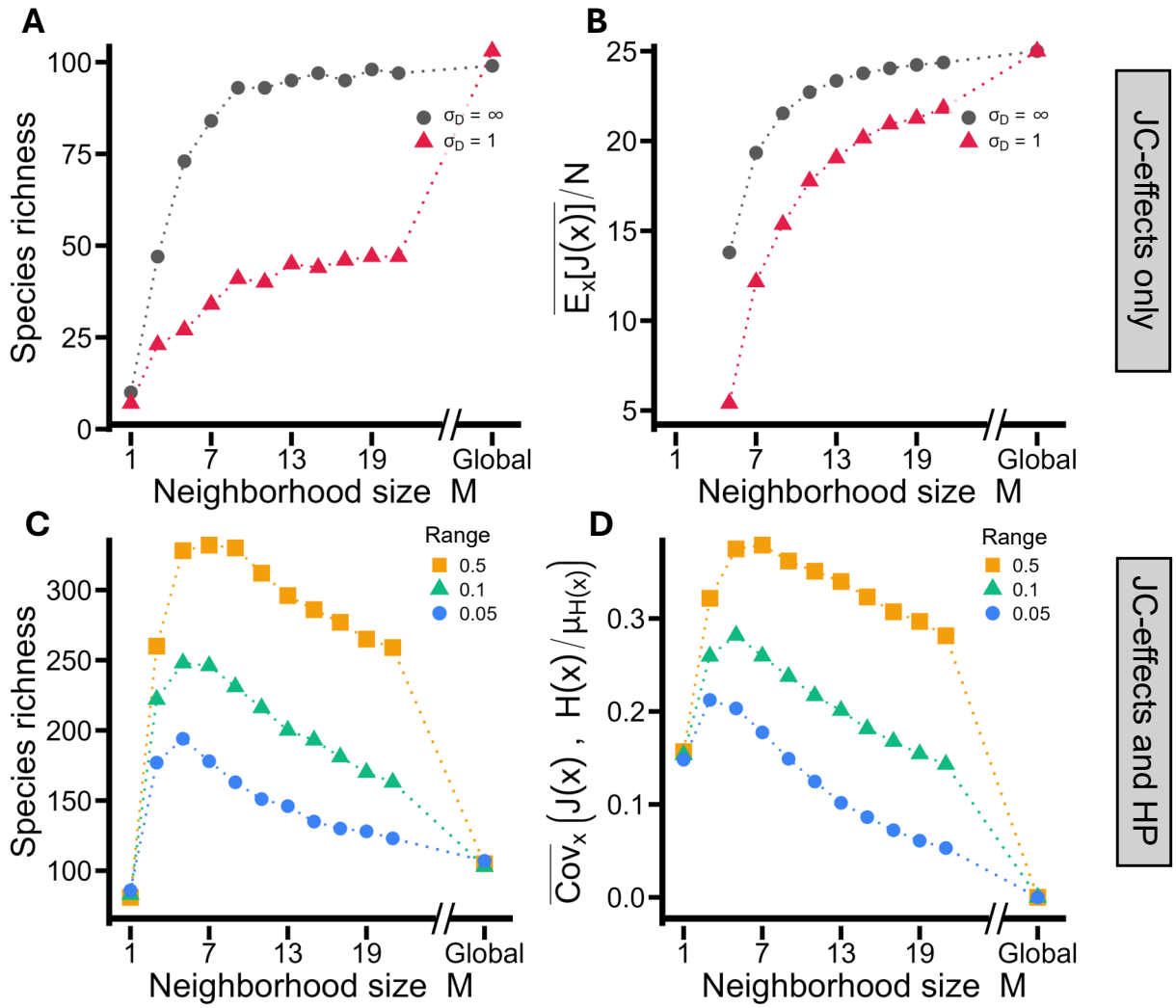

Figure 6: **The relationship between the spatial scale of JC-effects and species richness differs depending on whether JC–HP covariance is present.** Total JC-effect pressure was held constant ($aM^2 = K = 25$). (A) Species richness as a function of M with JC-effects alone under global dispersal ($\sigma_D = \infty$) and strong dispersal limitation ($\sigma_D = 1$). (B) The quantity $K\left(1 - \frac{K}{2M^2}\overline{\kappa}_M\right) = \overline{\mathbb{E}_x[J(x)]}/N$ as a function of M; $\overline{\kappa}_M$ was numerically calculated from simulations. Note values are truncated for small $M - a$ is large when M is small, which causes the approximation to fail. (C) Species richness as a function of M when JC-effects and habitat partitioning operate, for three habitat range values (nugget $= 0$). (D) JC–HP covariance as a function of M. All simulations used $\nu = 0.3 \times 10^{-5}$, $Y \sim \text{lognormal}(\mu = 0, \sigma_Y = 0.3)$; in (C,D), $\sigma_h = 0.02$.

The spatial scale of JC-effects and species richness

The relationship between the spatial scale of JC-effects (M) and species richness differed qualitatively depending on whether JC-effects occurred alone or alongside habitat partitioning, in simulations where the total JC-effect pressure was held constant ($aM^2 = K$). With JC-effects alone, species richness increased with M, saturating at a maximum value under global JC-effects (Fig. 6A). The increase in richness under global JC-effects was especially pronounced when species were dispersal limited (Fig. 6A, red triangles vs. gray circles).

These results follow directly from the expressions for stabilization due to JC-effects (equations 2 and 8). Given constant total JC-effects per tree ($aM^2 = K$), stabilization is proportional to

$$K\left(1 - \frac{K}{2M^2}\,\overline{\kappa}_M\right) \;=\; \frac{\overline{\mathbb{E}_x[J(x)]}}{N}.$$

This quantity is a strictly increasing, concave (saturating) function of M (Fig. 6B). Dispersal limitation increases $\overline{\kappa}_M$, thereby reducing $\overline{\mathbb{E}_x[J(x)]}/N$ (Fig. 6B, compare gray circles to red triangles). Thus, *direct* JC-effect strength is maximized when it occurs at larger spatial scales.

By contrast, species richness peaked at an intermediate spatial scale M when both JC-effects and habitat partitioning operated (assuming habitats were spatially autocorrelated; Fig. 6C). This occurs because the JC–HP covariance also peaked at intermediate M (Fig. 6D). When JC-effects extend over large spatial scales ($M > 5$ or $M > 7$; Fig. 6C), they spill over into relatively poor habitat types, reducing the JC–HP covariance. This decline is slower when spatial autocorrelation has a relatively large range of variation (Fig. 6C–D; compare orange to yellow and green points).

Discussion

Quantifying how coexistence mechanisms interact is crucial for understanding their consequences for species richness. I show that two leading explanations for tropical forest di-

versity—Janzen–Connell effects (JC-effects) and habitat partitioning (HP)—can interact in ways that fundamentally alter their outcomes. When habitat specialization causes species to cluster in environments where they perform best, JC-effects and HP act synergistically to promote high species richness. By contrast, aggregation arising from dispersal limitation undermines the ability of JC-effects to maintain coexistence.

Conceptual and theoretical context

JC-effects and habitat partitioning each face limitations when operating alone. JC-effects generate negative frequency dependence by reducing recruitment near conspecific adults, but their stabilizing effect declines with species richness ($\propto 1/N$) (Chisholm & Fung, 2020; Smith, 2022). Habitat partitioning allows species with different habitat preferences to coexist (Snyder & Chesson, 2003; Wright, 2002), yet its effect also decays with N and cannot sustain high richness unless niches are quite narrow.

When the two mechanisms act together, their interactions can greatly exceed the sum of their parts. In spatially autocorrelated habitats, species cluster in environments where they perform best, and resident adults disproportionately impose JC-effects on those same favorable locations. Invaders that share habitat preferences therefore encounter weakened competitors, because residents are heavily suppressed precisely where they would otherwise hold the strongest advantage. The strength of this interaction is captured by the JC–HP covariance, which decays more slowly with species richness ($\propto 1/\sqrt{N}$) than the direct effect of either mechanism ($\propto 1/N$), and so remains strong even in highly diverse communities. This allows habitat partitioning that might otherwise sustain only 10–30 species to maintain hundreds when coupled with JC-effects (Figs. 2G, 3B). While extreme parameter choices could in principle allow high richness under JC-effects alone (very large a and M) or habitat partitioning alone (very small σ_h), JC–HP interactions achieve the same outcome under far less restrictive conditions because their contribution to invasion erodes much more slowly with N.

This result builds on and contrasts with previous theory. Stump & Chesson (2015) analyzed a simplified case in which space was implicit and JC-effects operated only at the parent's patch, without explicit spatial structure. Under those assumptions, they found little interaction between JC-effects and habitat partitioning and argued that distance-dependent specialized predation is less able to promote coexistence than globally dispersing predators. I recover this outcome when only JC-effects operate (Fig. 6A–B). However, once habitat partitioning is included, the conclusion reverses: local, distance-dependent JC-effects strongly stabilize coexistence (Fig. 6C–D). This is because global JC-effects (e.g., globally dispersing natural enemies) do not generate a JC–HP covariance, whereas local effects do. Thus, when space is modeled explicitly, the *local* nature of JC-effects greatly amplifies their ability to promote coexistence in the presence of habitat partitioning and autocorrelated habitats.

JC–HP interactions can also be antagonistic. When habitat partitioning acts alone, dispersal limitation promotes coexistence because rare species disproportionately recruit into favorable habitats, generating a fitness–density covariance (Chesson, 2000a; Snyder, 2008). JC-effects can erode this fitness–density covariance by reducing conspecific recruitment in those favorable patches. Notably, interactions were antagonistic only under low autocorrelation (when habitat structure did not generate a JC–HP covariance) and when trees were dispersal limited (see Fig. 3C,G). Thus, whether JC–HP interactions are synergistic or antagonistic depends qualitatively on both habitat structure and dispersal.

Aggregation, JC-effects, and coexistence

The results of this study suggest the need to reinterpret the relationship between intraspecific aggregation, JC-effects, and coexistence. JC-effects are often associated with overdispersion (Janzen, 1970; Chave *et al.*, 2002; Wiegand & Moloney, 2013), which is commonly used as evidence of their strong operation. However, when habitat partitioning operates alongside JC-effects, species richness increases with intraspecific aggregation (Fig. 5G,L,P) through the JC–HP covariance. Thus, findings that habitat partitioning and dispersal limitation explain

spatial distributions more than JC-effects (e.g., Zhu *et al.*, 2013; Barry & Schnitzer, 2021) are not inconsistent with JC-effects contributing substantially to diversity maintenance (see also Kalyuzhny *et al.*, 2023).

The JC–HP interaction provides a more empirically plausible pathway to high diversity maintenance than JC-effects alone once spatial aggregation is taken into account. Chisholm & Fung (2020) argue that the close proximity of conspecific adults in sites such as the Barro Colorado Island (BCI) Forest Dynamics Plot makes it implausible that JC-effects are strong enough to fully prevent local recruitment. Consistent with this view, JC-effects on their own maintain substantial richness only when baseline strength a is very large; such values eliminate recruitment near adults (Fig. 5A) and generate pronounced overdispersion ($\overline{\kappa} < 1$; Fig. 5E,I,M). These patterns contrast sharply with those observed at BCI and the near-universal aggregation of tropical trees (Condit *et al.*, 2000). By contrast, the positive aggregation–richness relationship arising from the JC–HP covariance aligns with empirical aggregation patterns, indicating that widespread conspecific clustering is compatible with a substantial role for JC-effects in diversity maintenance.

Aggregation is not inherently indicative of strong or weak stabilization by JC-effects; its consequences depend on the processes that generate it. Habitat specialization promotes coexistence by concentrating JC-effects in favorable environments, whereas dispersal limitation undermines coexistence by reducing the average strength of JC-effects (equation 8) and preventing rare species' propagules from escaping conspecific effects. This result is consistent with some relatively recent theory (Stump & Chesson, 2015; Chisholm & Fung, 2020) although contrasts earlier work (Adler & Muller-Landau, 2005). Importantly, if dispersal limitation overrides the repulsion generated by JC-effects, it likely signals that JC-effects are weak and cannot maintain high richness (Fig. 5 J,N). In contrast, JC-effects too "weak" to prevent aggregation from habitat specialization can still sustain high richness through the JC–HP covariance.

Dispersal-based aggregation that decouples recruits from parent locations can enhance

coexistence (e.g. via animal dispersal Wiegand *et al.*, 2021, 2025); this form of dispersal limitation may interact with JC-effects and habitat partitioning in a different way.

Overall, documenting aggregation alone is insufficient for inferring the importance of JC-effects. Dispersal limitation and habitat specialization can generate superficially similar clustering patterns (Fig. 5J,N vs. L,P) but have qualitatively different implications for how JC-effects regulate species richness. Identifying the processes that generate aggregation is therefore essential to assess how spatial patterns relate to the efficacy of denstiy-dependent processes such as JC-effects.

Empirical considerations for forest communities

These theoretical results highlight a promising empirical target: directly measuring the JC–HP covariance in forest plots. The importance of habitat heterogeneity varies among sites (Shen *et al.*, 2013), and the strength of its interaction with local density dependence likely varies as well. For example, the BCI Forest Dynamics Plot in Panama was deliberately chosen for relatively low spatial heterogeneity (Hubbell *et al.*, 2024), whereas the Lambir Hills plot in Malaysia exhibits sharp edaphic contrasts, steep species turnover, and harbors roughly four times as many tree species in a comparable area (52 ha vs. 50 ha; Palmiotto *et al.*, 2004; Russo *et al.*, 2005). Stabilizing conspecific negative density dependence has been detected at both sites (Hülsmann *et al.*, 2024). Lambir Hills' higher richness may therefore reflect not habitat heterogeneity *per se*, but the way heterogeneity interacts with density-dependent processes such as JC-effects.

A key challenge is to quantify how variation in habitat heterogeneity among sites shapes the relative importance of JC-effects, habitat partitioning, and their interaction. This requires not only estimating the strength of each mechanism, but also identifying the processes that generate conspecific aggregation. Targeted approaches that disentangle density-dependent from habitat-associated effects are therefore essential. One promising direction is to extend generalized linear mixed models (GLMMs) and spatial point-pattern analyses to

incorporate environmental maps, enabling joint estimation of conspecific (and heterospecific) distance- and density-dependent effects alongside spatially varying abiotic factors (e.g., topography, elevation, soil chemistry; Yao *et al.*, 2020; Huang *et al.*, 2022; Wiegand & Moloney, 2013; Wiegand *et al.*, 2021). Because JC-effects and habitat partitioning are predicted to interact most strongly under positive spatial autocorrelation, captured by the JC–HP covariance, such methods offer a tractable way to quantify their joint contribution to coexistence.

Experimental manipulations provide a complementary approach. Factorial designs that cross conspecific proximity with fungicide treatments have already demonstrated the role of specialized pathogens in generating conspecific negative density dependence (Bagchi *et al.*, 2010, 2014; Liu *et al.*, 2012). Extending these experiments to include habitat variation would directly test the JC–HP interaction by asking whether natural enemies suppress seedlings most strongly in habitats where they would otherwise have high survival. In practice, this predicts a positive correlation between the increase in survival due to fungicide ($\Delta S_{\text{fungicide}}$) and baseline survival in the absence of enemies (S_{baseline}). Equivalently, this corresponds to $\text{Cov}(\Delta S_{\text{fungicide}}, S_{\text{baseline}}) > 0$, directly paralleling the JC–HP covariance term. Such designs would provide an empirical measure of the JC–HP covariance and its contribution to diversity maintenance.

Future directions and conclusion

Several simplifying assumptions in the model suggest avenues for extension. I considered a one-dimensional habitat axis, but real forests contain multiple abiotic gradients that vary independently and across scales (John *et al.*, 2007); extending the model to multidimensional environments would capture this complexity. Similarly, JC-effect strength was modeled as independent of habitat type, although evidence suggests that habitat variables can modify the baseline strength of density dependence (e.g. Yang *et al.*, 2023). Certain environments (e.g., moister habitats; Milici *et al.*, 2020) may therefore generate stronger JC–HP interactions. I also assumed natural enemies to be perfectly specialized, whereas spillover across

related species is common (Gilbert & Webb, 2007; Ødegaard *et al.*, 2005). Incorporating partial enemy overlap may alter JC–HP interactions depending on whether species that share habitat preferences also share natural enemies (see Stump, 2017). The coevolution of natural enemy specialization on host trees and tree habitat specialization (Fine *et al.*, 2004, 2013) is a particularly interesting avenue to explore in future models.

Functional traits such as seed size trade off with susceptibility to density dependence: larger-seeded species experience weaker CNDD (Lebrija-Trejos *et al.*, 2016). This axis of variation could be integrated into the tolerance–fecundity trade-off (see Supplementary Information; Muller-Landau, 2010; D'Andrea & O'Dwyer, 2021), helping connect the JC–HP mechanism to observed trait variation in tropical forests (but see Detto & Pacala, 2024). Interspecific variation in dispersal distances (Muller-Landau *et al.*, 2008) provides another avenue to link JC–HP interactions with life-history trade-offs (Stump & Comita, 2020). Together, these axes of variation could help embed JC–HP interactions into a broader trait-based framework.

While these extensions may yield further insights, the main result is likely robust: JC-effects and habitat partitioning are not independent forces but interact strongly through the spatial structure of forests. When habitats are spatially autocorrelated, habitat specialization generates conspecific aggregation in favorable environments, concentrating JC-effects where they matter most and producing a powerful mechanism for coexistence. By contrast, aggregation arising from dispersal limitation undermines coexistence. Thus, the consequences of aggregation depend critically on its underlying cause. Recognizing this distinction helps reconcile apparent contradictions in previous theory and highlights a clear path forward. Identifying and quantifying the processes that generate spatial patterns, and integrating these with process-based theory, will be essential for linking local dynamics to the maintenance of community-level biodiversity. This integration offers a tractable way to connect spatial data from forest plots and experiments with theoretical predictions, providing a concrete framework to test how local processes scale to sustain tropical forest diversity.

Data availability

All code required to reproduce the analyses and results in this paper is available at: https://github.com/DanielSmithEcology/Janzen_Connell_Habitat_Partitioning_Interactions.

Acknowledgements

This research was funded by the U.S. National Science Foundation grant NSF OCE 1851489 and National Science Foundation Division of Environmental Biology Award 2240430. I thank J. Timothy Wootton, Catherine A Pfister, Mercedes Pascual, Trevor Price, Lukas Magee, and the Wootton-Pfister lab for insightful discussion and feedback on the manuscript.

References

Adler, F.R. & Muller-Landau, H.C. (2005). When do localized natural enemies increase species richness? *Ecology Letters*, 8, 438–447.

Andersen, K.M., Turner, B.L. & Dalling, J.W. (2010). Soil-based habitat partitioning in understorey palms in lower montane tropical forests. *Journal of biogeography*, 37, 278–292.

Armstrong, R.A. & McGehee, R. (1980). Competitive exclusion. *The American Naturalist*, 115, 151–170.

Bagchi, R., Gallery, R.E., Gripenberg, S., Gurr, S.J., Narayan, L., Addis, C.E., Freckleton, R.P. & Lewis, O.T. (2014). Pathogens and insect herbivores drive rainforest plant diversity and composition. *Nature*, 506, 85–88.

Bagchi, R., Henrys, P.A., Brown, P.E., Burslem, D.F.P., Diggle, P.J., Gunatilleke, C.S., Gunatilleke, I.N., Kassim, A.R., Law, R., Noor, S. *et al.* (2011). Spatial patterns reveal

negative density dependence and habitat associations in tropical trees. *Ecology*, 92, 1723–1729.

Bagchi, R., Swinfield, T., Gallery, R.E., Lewis, O.T., Gripenberg, S., Narayan, L. & Freckleton, R.P. (2010). Testing the janzen-connell mechanism: Pathogens cause overcompensating density dependence in a tropical tree. *Ecology letters*, 13, 1262–1269.

Bai, X., Queenborough, S.A., Wang, X., Zhang, J., Li, B., Yuan, Z., Xing, D., Lin, F., Ye, J. & Hao, Z. (2012). Effects of local biotic neighbors and habitat heterogeneity on tree and shrub seedling survival in an old-growth temperate forest. *Oecologia*, 170, 755–765.

Baldeck, C.A., Harms, K.E., Yavitt, J.B., John, R., Turner, B.L., Valencia, R., Navarrete, H., Davies, S.J., Chuyong, G.B., Kenfack, D. *et al.* (2013). Soil resources and topography shape local tree community structure in tropical forests. *Proceedings of the Royal Society B: Biological Sciences*, 280, 20122532.

Barry, K.E. & Schnitzer, S.A. (2021). Are we missing the forest for the trees? conspecific negative density dependence in a temperate deciduous forest. *Plos one*, 16, e0245639.

Bezanson, J., Edelman, A., Karpinski, S. & Shah, V.B. (2017). Julia: A fresh approach to numerical computing. *SIAM Review*, 59, 65–98.

Bolker, B.M., Pacala, S.W. & Neuhauser, C. (2003). Spatial dynamics in model plant communities: what do we really know? *The American Naturalist*, 162, 135–148.

Brown, C., Burslem, D., Illian, J., Bao, L., Brockelman, W., Cao, M., Chang, L., Dattaraja, H., Davies, S., Gunatilleke, C. *et al.* (2013). Multispecies coexistence of trees in tropical forests: spatial signals of topographic niche differentiation increase with environmental heterogeneity. *Proceedings of the Royal Society B: Biological Sciences*, 280, 20130502.

Cao, J., Zhang, C., Zhao, B., Li, X., Hou, M. & Zhao, X. (2018). Seedling density dependence

regulated by population density and habitat filtering: Evidence from a mixed primary broad-leaved korean pine forest in northeastern china. *Annals of Forest Science*, 75, 25.

Chave, J., Muller-Landau, H.C. & Levin, S.A. (2002). Comparing classical community models: theoretical consequences for patterns of diversity. *The American Naturalist*, 159, 1–23.

Chen, L., Mi, X., Comita, L.S., Zhang, L., Ren, H. & Ma, K. (2010). Community-level consequences of density dependence and habitat association in a subtropical broad-leaved forest. *Ecology letters*, 13, 695–704.

Chesson, P. (2000a). General theory of competitive coexistence in spatially-varying environments. *Theoretical population biology*, 58, 211–237.

Chesson, P. (2000b). Mechanisms of maintenance of species diversity. *Annual review of Ecology and Systematics*, 31, 343–366.

Chesson, P. (2003). Quantifying and testing coexistence mechanisms arising from recruitment fluctuations. *Theoretical population biology*, 64, 345–357.

Chesson, P. & Neuhauser, C. (2002). Intraspecific aggregation and species coexistence. *Trends in Ecology & Evolution*, 17, 210–211.

Chisholm, R.A. & Fung, T. (2020). Janzen-connell effects are a weak impediment to competitive exclusion. *The American Naturalist*, 196, 649–661.

Comita, L.S., Aguilar, S., Pérez, R., Lao, S. & Hubbell, S.P. (2007). Patterns of woody plant species abundance and diversity in the seedling layer of a tropical forest. *Journal of Vegetation science*, 18, 163–174.

Comita, L.S., Muller-Landau, H.C., Aguilar, S. & Hubbell, S.P. (2010). Asymmetric density dependence shapes species abundances in a tropical tree community. *Science*, 329, 330–332.

Comita, L.S., Queenborough, S.A., Murphy, S.J., Eck, J.L., Xu, K., Krishnadas, M., Beckman, N. & Zhu, Y. (2014). Testing predictions of the janzen–connell hypothesis: a meta-analysis of experimental evidence for distance-and density-dependent seed and seedling survival. *Journal of Ecology*, 102, 845–856.

Condit, R., Ashton, P.S., Baker, P., Bunyavejchewin, S., Gunatilleke, S., Gunatilleke, N., Hubbell, S.P., Foster, R.B., Itoh, A., LaFrankie, J.V. *et al.* (2000). Spatial patterns in the distribution of tropical tree species. *Science*, 288, 1414–1418.

Cressie, N.A.C. (1993). *Statistics for Spatial Data*. Revised edn. Wiley, New York.

Dalling, J.W., Muller-Landau, H.C., Wright, S.J. & Hubbell, S.P. (2002). Role of dispersal in the recruitment limitation of neotropical pioneer species. *Journal of Ecology*, 90, 714–727.

Detto, M. & Muller-Landau, H.C. (2013). Fitting ecological process models to spatial patterns using scalewise variances and moment equations. *The American Naturalist*, 181, E68–E82.

Detto, M. & Pacala, S. (2024). Integrating conspecifics negative density dependence, successional and evolutionary dynamics: Towards a theory of forest diversity. *Communications Biology*, 7, 1572.

Detto, M., Visser, M.D., Wright, S.J. & Pacala, S.W. (2019). Bias in the detection of negative density dependence in plant communities. *Ecology Letters*, 22, 1923–1939.

D'Andrea, R., Barabás, G. & Ostling, A. (2013). Revising the tolerance-fecundity trade-off; or, on the consequences of discontinuous resource use for limiting similarity, species diversity, and trait dispersion. *The American Naturalist*, 181, E91–E101.

D'Andrea, R. & O'Dwyer, J.P. (2021). Competition for space in a structured landscape: The effect of seed limitation on coexistence under a tolerance-fecundity trade-off. *Journal of Ecology*, 109, 1886–1897.

Feng, Z., Wu, J., Sun, J., Yu, X., Wang, L., Chen, F. & Hu, X. (2023). Habitat filtering covers the strength of density dependence and functional density dependence on seedling survival in cangshan mountain, southwest china. *Forests*, 15, 76.

Fine, P.V., Mesones, I. & Coley, P.D. (2004). Herbivores promote habitat specialization by trees in amazonian forests. *science*, 305, 663–665.

Fine, P.V., Metz, M.R., Lokvam, J., Mesones, I., ZUNiga, J.M.A., Lamarre, G.P., Pilco, M.V. & Baraloto, C. (2013). Insect herbivores, chemical innovation, and the evolution of habitat specialization in amazonian trees. *Ecology*, 94, 1764–1775.

Fortunel, C., Lasky, J.R., Uriarte, M., Valencia, R., Wright, S.J., Garwood, N.C. & Kraft, N.J. (2018). Topography and neighborhood crowding can interact to shape species growth and distribution in a diverse amazonian forest. *Ecology*, 99, 2272–2283.

Freckleton, R.P. & Lewis, O.T. (2006). Pathogens, density dependence and the coexistence of tropical trees. *Proceedings of the Royal Society B: Biological Sciences*, 273, 2909–2916.

Gilbert, G.S. & Webb, C.O. (2007). Phylogenetic signal in plant pathogen–host range. *Proceedings of the National Academy of Sciences*, 104, 4979–4983.

Hardin, G. (1960). The competitive exclusion principle: an idea that took a century to be born has implications in ecology, economics, and genetics. *science*, 131, 1292–1297.

Huang, T.H., Huang, C.L., Lin, Y.C. & Sun, I.F. (2022). Seedling survival simultaneously determined by conspecific, heterospecific, and phylogenetically related neighbors and habitat heterogeneity in a subtropical forest in taiwan. *Ecology and Evolution*, 12, e8525.

Hubbell, S.P., Ahumada, J.A., Condit, R. & Foster, R.B. (2001). Local neighborhood effects on long-term survival of individual trees in a neotropical forest. *Ecological Research*, 16, 859–875.

Hubbell, S.P., Foster, R.B. & Rubinoff, I. (2024). Early history of the barro colorado island forest dynamics project. In: *The First 100 Years of Research on Barro Colorado: Plant and Ecosystem Science (Volumes 1 and 2)* (eds. Muller-Landau, H.C. & Wright, S.J.). Smithsonian Institution Scholarly Press, Washington, D.C.

Hülsmann, L., Chisholm, R.A., Comita, L., Visser, M.D., de Souza Leite, M., Aguilar, S., Anderson-Teixeira, K.J., Bourg, N.A., Brockelman, W.Y., Bunyavejchewin, S. *et al.* (2024). Latitudinal patterns in stabilizing density dependence of forest communities. *Nature*, 627, 564–571.

Hyatt, L.A., Rosenberg, M.S., Howard, T.G., Bole, G., Fang, W., Anastasia, J., Brown, K., Grella, R., Hinman, K., Kurdziel, J.P. *et al.* (2003). The distance dependence prediction of the janzen-connell hypothesis: a meta-analysis. *Oikos*, 103, 590–602.

Janzen, D.H. (1970). Herbivores and the number of tree species in tropical forests. *The American Naturalist*, 104, 501–528.

Jensen, J.L.W.V. (1906). Sur les fonctions convexes et les inégalités entre les valeurs moyennes. *Acta mathematica*, 30, 175–193.

John, R., Dalling, J.W., Harms, K.E., Yavitt, J.B., Stallard, R.F., Mirabello, M., Hubbell, S.P., Valencia, R., Navarrete, H., Vallejo, M. *et al.* (2007). Soil nutrients influence spatial distributions of tropical tree species. *Proceedings of the National Academy of Sciences*, 104, 864–869.

Johnson, D.J., Bourg, N.A., Howe, R., McShea, W.J., Wolf, A. & Clay, K. (2014). Conspecific negative density-dependent mortality and the structure of temperate forests. *Ecology*, 95, 2493–2503.

Johnson, D.J., Condit, R., Hubbell, S.P. & Comita, L.S. (2017). Abiotic niche partitioning and negative density dependence drive tree seedling survival in a tropical forest. *Proceedings of the Royal Society B: Biological Sciences*, 284, 20172210.

Jones, M.M., Szyska, B. & Kessler, M. (2011). Microhabitat partitioning promotes plant diversity in a tropical montane forest. *Global Ecology and Biogeography*, 20, 558–569.

Kalyuzhny, M., Lake, J.K., Wright, S.J. & Ostling, A.M. (2023). Pervasive within-species spatial repulsion among adult tropical trees. *Science*, 381, 563–568.

Lebrija-Trejos, E., Reich, P.B., Hernández, A. & Wright, S.J. (2016). Species with greater seed mass are more tolerant of conspecific neighbours: a key driver of early survival and future abundances in a tropical forest. *Ecology letters*, 19, 1071–1080.

Levi, T., Barfield, M., Barrantes, S., Sullivan, C., Holt, R.D. & Terborgh, J. (2019). Tropical forests can maintain hyperdiversity because of enemies. *Proceedings of the National Academy of Sciences*, 116, 581–586.

Levin, S.A. (1970). Community equilibria and stability, and an extension of the competitive exclusion principle. *The American Naturalist*, 104, 413–423.

Levine, J.M. & HilleRisLambers, J. (2009). The importance of niches for the maintenance of species diversity. *Nature*, 461, 254–257.

Liu, H., Xie, F., Shi, H., Shu, X., Zhang, K., Zhang, Q. & Dang, H. (2022). Disentangling the effects of biotic neighbors and habitat heterogeneity on seedling survival in a deciduous broad-leaved forest. *Forest Ecology and Management*, 519, 120339.

Liu, X., Liang, M., Etienne, R.S., Wang, Y., Staehelin, C. & Yu, S. (2012). Experimental evidence for a phylogenetic janzen–connell effect in a subtropical forest. *Ecology letters*, 15, 111–118.

Lu, J., Johnson, D.J., Qiao, X., Lu, Z., Wang, Q. & Jiang, M. (2015). Density dependence and habitat preference shape seedling survival in a subtropical forest in central china. *Journal of Plant Ecology*, 8, 568–577.

Magee, L., Wolf, A., Howe, R., Schubbe, J., Hagenow, K. & Turner, B. (2021). Density dependence and habitat heterogeneity regulate seedling survival in a north american temperate forest. *Forest Ecology and Management*, 480, 118722.

Mangan, S.A., Schnitzer, S.A., Herre, E.A., Mack, K.M., Valencia, M.C., Sanchez, E.I. & Bever, J.D. (2010). Negative plant–soil feedback predicts tree-species relative abundance in a tropical forest. *Nature*, 466, 752.

Milici, V.R., Dalui, D., Mickley, J.G. & Bagchi, R. (2020). Responses of plant–pathogen interactions to precipitation: Implications for tropical tree richness in a changing world. *Journal of Ecology*, 108, 1800–1809.

Moles, A.T., Warton, D.I. & Westoby, M. (2003). Do small-seeded species have higher survival through seed predation than large-seeded species? *Ecology*, 84, 3148–3161.

Moles, A.T. & Westoby, M. (2004). Seedling survival and seed size: a synthesis of the literature. *Journal of Ecology*, 92, 372–383.

Muller-Landau, H. (2010). The tolerance–fecundity trade-off and the maintenance of diversity in seed size. *Proceedings of the National Academy of Sciences*, 107, 4242–4247.

Muller-Landau, H.C., Wright, S.J., Calderón, O., Condit, R. & Hubbell, S.P. (2008). Interspecific variation in primary seed dispersal in a tropical forest. *Journal of Ecology*, pp. 653–667.

Murrell, D., Purves, D. & Law, R. (2002). Intraspecific aggregation and species coexistence. *Trends in Ecology & Evolution*, 17, 211.

Ødegaard, F., Diserud, O.H. & Østbye, K. (2005). The importance of plant relatedness for host utilization among phytophagous insects. *Ecology Letters*, 8, 612–617.

Palmiotto, P.A., Davies, S.J., Vogt, K.A., Ashton, M.S., Vogt, D.J. & Ashton, P.S. (2004).

Soil-related habitat specialization in dipterocarp rain forest tree species in borneo. *Journal of Ecology*, pp. 609–623.

Piao, T., Comita, L.S., Jin, G. & Kim, J.H. (2013). Density dependence across multiple life stages in a temperate old-growth forest of northeast china. *Oecologia*, 172, 207–217.

Potts, M.D., Ashton, P.S., Kaufman, L.S. & Plotkin, J.B. (2002). Habitat patterns in tropical rain forests: a comparison of 105 plots in northwest borneo. *Ecology*, 83, 2782–2797.

Pu, X., Zhu, Y. & Jin, G. (2017). Effects of local biotic neighbors and habitat heterogeneity on seedling survival in a spruce-fir valley forest, northeastern china. *Ecology and evolution*, 7, 4582–4591.

Queenborough, S.A., Burslem, D.F., Garwood, N.C. & Valencia, R. (2009). Taxonomic scale-dependence of habitat niche partitioning and biotic neighbourhood on survival of tropical tree seedlings. *Proceedings of the Royal Society B: Biological Sciences*, 276, 4197–4205.

R Core Team (2021). *R: A Language and Environment for Statistical Computing*. R Foundation for Statistical Computing, Vienna, Austria.

Ripley, B.D. (1976). The second-order analysis of stationary point processes. *Journal of applied probability*, 13, 255–266.

Robbe, P. (2023). *GaussianRandomFields.jl Documentation*. Documenter.jl. Version 0.27.24, generated on 23 May 2023.

Russo, S.E., Davies, S.J., King, D.A. & Tan, S. (2005). Soil-related performance variation and distributions of tree species in a bornean rain forest. *Journal of Ecology*, 93, 879–889.

Shen, G., He, F., Waagepetersen, R., Sun, I.F., Hao, Z., Chen, Z.S. & Yu, M. (2013). Quantifying effects of habitat heterogeneity and other clustering processes on spatial distributions of tree species. *Ecology*, 94, 2436–2443.

Silvertown, J. (2004). Plant coexistence and the niche. *Trends in Ecology & evolution*, 19, 605–611.

Smith, D.J. (2022). The functional form of specialised predation affects whether janzen–connell effects can prevent competitive exclusion. *Ecology Letters*.

Snyder, R.E. (2008). When does environmental variation most influence species coexistence? *Theoretical Ecology*, 1, 129–139.

Snyder, R.E. & Chesson, P. (2003). Local dispersal can facilitate coexistence in the presence of permanent spatial heterogeneity. *Ecology letters*, 6, 301–309.

Song, X., Lim, J.Y., Yang, J. & Luskin, M.S. (2021). When do janzen–connell effects matter? a phylogenetic meta-analysis of conspecific negative distance and density dependence experiments. *Ecology Letters*, 24, 608–620.

Stein, A., Gerstner, K. & Kreft, H. (2014). Environmental heterogeneity as a universal driver of species richness across taxa, biomes and spatial scales. *Ecology letters*, 17, 866–880.

Stump, S.M. (2017). Multispecies coexistence without diffuse competition; or, why phylogenetic signal and trait clustering weaken coexistence. *The American Naturalist*, 190, 213–228.

Stump, S.M. & Chesson, P. (2015). Distance-responsive predation is not necessary for the janzen–connell hypothesis. *Theoretical population biology*, 106, 60–70.

Stump, S.M. & Comita, L.S. (2020). Differences among species in seed dispersal and conspecific neighbor effects can interact to influence coexistence. *Theoretical Ecology*, pp. 1–31.

Terborgh, J.W. (2015). Toward a trophic theory of species diversity. *Proceedings of the National Academy of Sciences*, 112, 11415–11422.

Umarani, M.S., Wang, D., O'Dwyer, J.P. & D'Andrea, R. (2024). A spatial signal of niche differentiation in tropical forests. *The American Naturalist*, 203, 000–000.

Uriarte, M., Condit, R., Canham, C.D. & Hubbell, S.P. (2004). A spatially explicit model of sapling growth in a tropical forest: does the identity of neighbours matter? *Journal of Ecology*, 92, 348–360.

Wiegand, T. & Moloney, K.A. (2013). *Handbook of spatial point-pattern analysis in ecology.* CRC press.

Wiegand, T., Wang, X., Anderson-Teixeira, K.J., Bourg, N.A., Cao, M., Ci, X., Davies, S.J., Hao, Z., Howe, R.W., Kress, W.J. *et al.* (2021). Consequences of spatial patterns for coexistence in species-rich plant communities. *Nature Ecology & Evolution*, pp. 1–9.

Wiegand, T., Wang, X., Fischer, S.M., Kraft, N.J., Bourg, N.A., Brockelman, W.Y., Cao, G., Cao, M., Chanthorn, W., Chu, C. *et al.* (2025). Latitudinal scaling of aggregation with abundance and coexistence in forests. *Nature*, pp. 1–7.

Wright, J.S. (2002). Plant diversity in tropical forests: a review of mechanisms of species coexistence. *Oecologia*, 130, 1–14.

Wright, S.J., Muller-Landau, H.C., Calderón, O. & Hernandéz, A. (2005). Annual and spatial variation in seedfall and seedling recruitment in a neotropical forest. *Ecology*, 86, 848–860.

Wu, J., Swenson, N.G., Brown, C., Zhang, C., Yang, J., Ci, X., Li, J., Sha, L., Cao, M. & Lin, L. (2016). How does habitat filtering affect the detection of conspecific and phylogenetic density dependence? *Ecology*, 97, 1182–1193.

Yang, L., Johnson, D.J., Yang, Z., Yang, X., Yin, Q., Luo, Y., Hao, Z. & Jia, S. (2023). Trees species' dispersal mode and habitat heterogeneity shape negative density dependence in a temperate forest. *Forest Ecosystems*, 10, 100139.

Yao, J., Bachelot, B., Meng, L., Qin, J., Zhao, X. & Zhang, C. (2020). Abiotic niche partitioning and negative density dependence across multiple life stages in a temperate forest in northeastern china. *Journal of Ecology*, 108, 1299–1310.

Zhu, Y., Getzin, S., Wiegand, T., Ren, H. & Ma, K. (2013). The relative importance of janzen-connell effects in influencing the spatial patterns at the gutianshan subtropical forest. *PloS one*, 8, e74560.